Microstructural and Superconducting Radiofrequency Properties of Multilayer Sequentially Sputtered Nb_3Sn films

M. N. Sayeed, G.V. Eremeev, P. Owen, C. E. Reece, and H. E. Elsayed-Ali

***Abstract*— Nb_3Sn is considered as a potential candidate for superconducting radiofrequency cavities for particle acceleration due to its higher transition temperature of 18.3 K and higher superheating field of 400 mT. Nb_3Sn films can be grown inside the surface of a Nb cavity by sequentially sputtering multiple layers of Nb and Sn thin films followed by annealing at 950 °C for 3 h. We report on the properties of Nb_3Sn films grown on Nb substrates by magnetron sputtering. The films' crystal structure, surface morphology, and composition were characterized by X-ray diffraction, scanning electron microscopy, and energy-dispersive X-ray spectroscopy. The films had polycrystalline Nb_3Sn structure with fine grain surface and an atomic Sn composition of ~23%. The RF surface resistance of the films was measured for different temperatures at 7.4 GHz to understand the feasibility of this method for the SRF application. The RF surface resistance was 5 mΩ at 12 K, which is about 2 orders of magnitude higher than 60 μΩ previously measured in Nb_3Sn films grown by Sn vapor diffusion. The sputtered film had a superconducting transition at 17.2 K, which is also lower than 17.9 K observed in Nb_3Sn film prepared by vapor diffusion.**

***Index Terms*—multilayer sputtering, Nb_3Sn, superconducting radiofrequency, RF surface resistance, thin film.**

I. Introduction

SUPERCONDUCTING radiofrequency (SRF) cavities, which are one of the building blocks of particle accelerators and current accelerator technology, uses niobium as the sheet material of the SRF cavities [1]. However, niobium-based cavities are approaching the material-dependent limits (transition temperature T_c of 9.25 K, higher superheating field H_{sh} of 200 mT) [2]. Nb_3Sn is considered as a potential alternative of niobium cavities due to its better superconducting properties (T_c = 18.3 K, $H_{sh} \approx$ 400 mT) [3]. The better superconducting properties make it possible for Nb_3Sn SRF cavities to be operated efficiently at 4.2 K instead of the conventional 2 K for niobium cavities and can reduce the operating cost. However, Nb_3Sn cannot be used directly to fabricate a cavity due to the fragile nature of the material. The use of Nb_3Sn thin films inside of niobium or copper cavities are considered. Currently, Nb_3Sn films are fabricated inside single cell and multicell cavities by Sn vapor diffusion [1, 4-6]. Magnetron sputtering is considered as a potential alternative to fabricate Nb_3Sn SRF cavities [7-10].

While previous studies focused mainly on the structural and DC superconducting properties of the films, we focus on measuring RF surface resistance and transition temperature of the films. The main goal of this study is to understand the film applicability in SRF cavities.

This work was supported by the U.S. Department of Energy, Office of Science, Office of Nuclear Physics under Contract No. DE-AC05-06OR23177

(Corresponding author: Md Nizam Sayeed.)

M. N. Sayeed and H. E. Elsayed-Ali are with the department of Electrical and Computer Engineering, Old Dominion University, Norfolk, VA 23529, (e-mail: msaye004@odu.edu, helsayed@odu.edu).

P. Owen and C. E. Reece are with the Thomas Jefferson National Accelerator Facility, Newport News, VA 23606, USA (e-mail: powen@jlab.org, reece@jlab.org)

G. V. Eremeev is with Fermi National Accelerator Laboratory, Batavia, IL 60510, USA. (e-mail: grigory@fnal.gov).

Color versions of one or more of the figures in this paper are available online at http://ieeexplore.ieee.org.

II. Experiments

A. Sample Preparation

The Nb substrates were made from Nb sheets of high residual resistivity ratio (RRR ~250) which is typically used for SRF cavity fabrication. The substrates were cleaned by removing 100 μm using buffer chemical polishing (1:1:1 volume ratio of 49% HF, 70% HNO_3 and 85% H_3PO_4) and baked at 800 °C for 2 h in a vacuum furnace. The substrates were further cleaned by etching an additional 25 μm before the deposition.

Nb_3Sn films were fabricated in two steps: first multilayers of Nb and Sn films were deposited on a Nb substrate of 2-inch diameter by magnetron sputtering. The Nb and Sn targets were connected respectively to a DC power source and an RF power source in an AJA ATC Orion 5 commercial sputter coater. The deposition chamber was evacuated to ~10^{-7} Torr before the deposition. The thickness of alternating Nb and Sn layers were 20 and 10 nm, respectively. The Nb and Sn layers were repeated 100 times to get a 3 μm thick multilayer. The final layer was Nb to block Sn evaporation from the surface during the annealing. In the second step, the Nb-Sn multilayered films were annealed at 950 °C for 3 h in a separate vacuum furnace. The pressure inside the furnace during the annealing was ~10^{-5} Torr.

This manuscript has been authored by Fermi Research Alliance, LLC under Contract No. DE-AC02-07CH11359 with the U.S. Department of Energy, Office of Science, Office of High Energy Physics.

B. Sample Characterization

The film structure was characterized by a Rigaku Miniflex II X-ray diffractometer. X-ray diffraction patterns of the films were obtained using Cu-Kα radiation at a θ-2θ range of 20-100°. The surface morphology of the films were characterized by Hitachi S4700 Field Emission Scanning Electron Microscope (FESEM). Atomic composition of the films was measured by energy dispersive X-ray spectroscope (EDS).

The sample was loaded into the Surface Impedance Characterization (SIC) system at Jefferson lab. The system can measure the loaded quality factor Q_L and RF surface resistance R_s of superconducting films exposed to RF fields at 7.4 GHz down to cryogenic temperature. The SIC system details are described elsewhere [11].

III. Film Properties

Fig. 1 shows the X-ray diffraction patterns of the Nb-Sn multilayered film after annealing. The diffraction peaks correspond to Nb_3Sn (110), (200), (210), (211), (222), (320), (321), (400), (420), (421), and (332) diffraction orders. Two diffraction peaks of Nb (200) and Nb (310) are from the substrate. The absence of any diffraction peak due to Sn confirmed the intermetallic compound formation after annealing. Since Nb and Sn form two more intermetallic compounds (Nb_6Sn_5, $NbSn_2$) of low transition temperature, the diffraction data were matched for those compounds also. The film did not exhibit any diffraction peak due to Nb_6Sn_5 and $NbSn_2$.

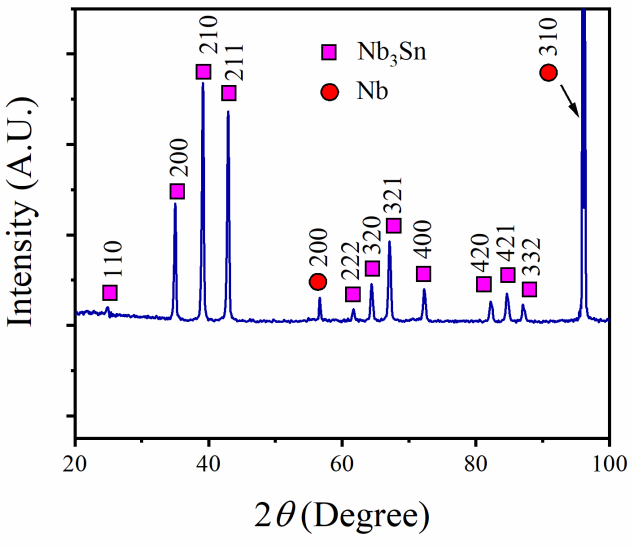

Fig. 1. XRD patterns of Nb-Sn multilayered films after annealing at 950 °C for 3 h. Most of the diffraction peaks correspond to the diffraction due to Nb_3Sn.

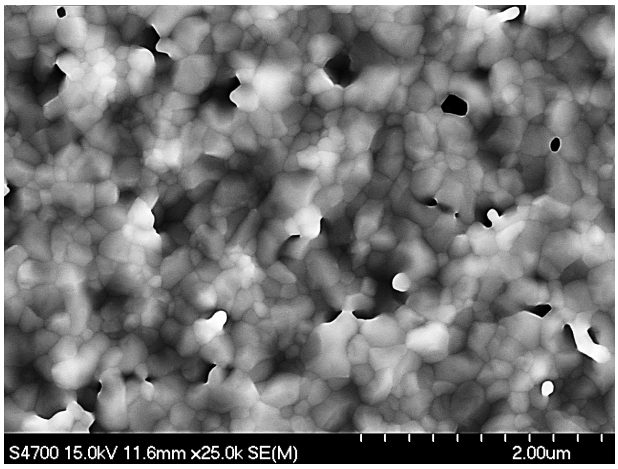

Fig. 2. FESEM image of the Nb_3Sn film fabricated by multilayer sputtering.

The film morphology obtained by the FESEM in Fig. 2 shows densely packed grain morphology. The grain size of the film was in the range of 100-300 nm. There were randomly distributed voids of ~200 nm throughout the whole surface. The atomic composition of Sn, measured from EDS on a surface area of 1.2 mm^2, was ~23%, whereas the as-deposited multilayered films had ~27% Sn. Our previous experiment on the effect of annealing temperature and multilayer thickness showed that, Sn loss is the result of the competition between the evaporation from the surface and diffusion in the bulk, with this competition depended on the annealing temperature [12,13].

IV. Superconducting Properties

A. Transition Temperature of the film

The transition temperature of the sample was measured from the loaded quality factor Q_L of the cavity as a function of sample temperature using Agilent's FieldFox N9915A network analyzer. The loaded quality factor was estimated by 3 dB technique using the following formula [14]:

$$Q_L = \frac{f_0}{|f^{+(-3dB)} - f^{-(-3dB)}|} \quad (1)$$

Where, f_0 and $f^{(-3dB)}$ are the resonant frequency of the cavity and the half-transmitted power frequency, respectively. The resulted loaded quality factor as a function of sample temperature is shown in Fig. 3. The loaded Q_L value dropped gradually with increasing sample temperature until it reached the T_c of the film. The film exhibited a T_c of 17.2 K. Above this temperature, the Q_L value remained almost constant.

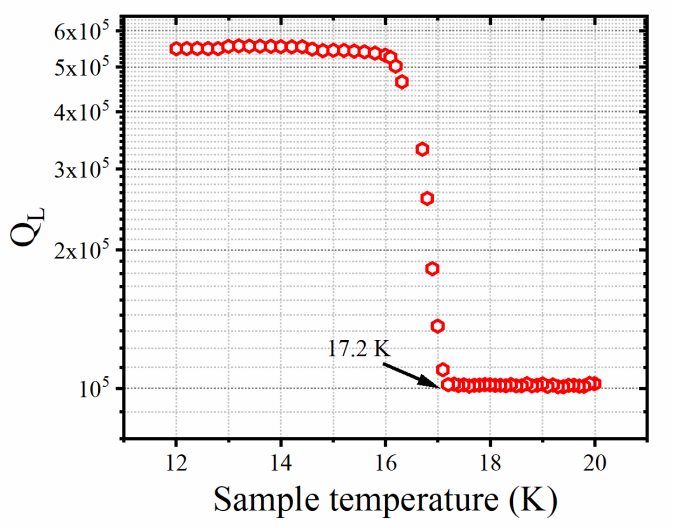

Fig. 3. Loaded quality factor Q_L as a function of sample temperature of the film.

B. *Surface Resistance of the Film*

The SIC system implements power compensation technique to measure the RF surface resistance of the film. The temperature of sample under investigation was controlled by a heater which is placed underneath the sample holder, whereas the whole cavity remained typically at 2 K. The heater keeps the sample temperature constant when an RF field is applied. Power dissipated into the film surface due to the RF field can be calculated from the difference of the heater power required to keep the sample at constant temperature with or without the RF field [15]:

$$P_{RF}\left(H_{peak}T_{sample}\right) = P_{heater}^{H=0;T=T_{sample}} - P_{heater}^{H=H_{peak};T=T_{sample}} \quad (2)$$

Finally, RF surface resistance R_{RF} of the film was measured from the dissipated power by [15]:

$$R_{RF}\left(H_{peak}T_{sample}\right) = \frac{P_{RF}\left(H_{peak}T_{sample}\right)}{k \cdot H_{peak}^2} \quad (3)$$

where, K is a geometry dependent constant found with numerical simulations [14,15] and H_{peak} is the peak magnetic field on the film surface. Fig. 4 shows the RF surface resistance of the sputtered film as a function of sample temperature. The surface resistance of a Nb_3Sn film fabricated by Sn vapor diffusion method in the same system is also plotted for reference.

The measured surface resistance has temperature dependent BCS surface resistance and temperature independent residual resistance. At 12 K, the residual resistance of the sputtered Nb_3Sn film was ~5 mΩ, whereas the vapor diffuse sample exhibited residual resistance of ~60 μΩ. The sputtered sample had a superconducting transition temperature lower than that of the vapor diffused sample. The inset of Fig. 4 shows the BCS portion of the surface resistance fitted by the SRIMP code by Jurgen Halbritter [16]. With constant fitting parameters coherence length ξ_0= 7 nm and mean free path = 3.10 nm, the residual resistance and the superconducting gap Δ obtained from the fit were 3.87 ± 0.28 mΩ and 2.52 ± 0.96 meV respectively.

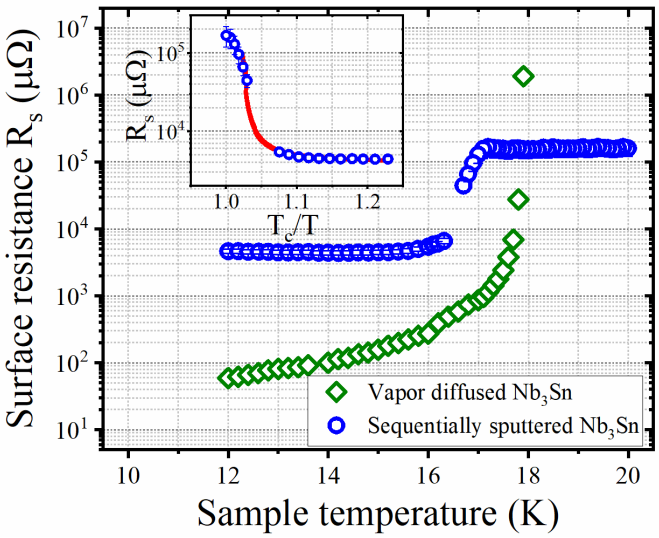

Fig. 4. RF surface resistance as a function of sample temperature of the sputtered (blue circle) and vapor diffused (green diamond) Nb_3Sn films. The inset shows the BCS fit of the sputtered sample. The data for the vapor diffused sample was obtained from [15].

V. Discussion

The superconducting T_c and gap of Nb_3Sn films depend on the atomic composition of Sn present on the films [17]. Sn composition on the sputtered film was less than standard composition of 25%. As a result, the RF superconducting T_c of the sputtered Nb_3Sn film was lower than that of the vapor diffused Nb_3Sn film. Based on the relationship between the superconducting T_c and gap with the Sn composition as reported by Godeke et al. [17], the Sn composition of the film should be ~24% to achieve a T_c ~17 K and a superconducting gap ~2.50 meV. The Sn composition of the sputtered film was ~23% as obtained from EDS. Note that, the depth resolution of EDS is limited; for 15 keV electron, the X-ray transmission fraction for Nb-Lα and Sn-Lα lines are smaller than the thickness of the film. The residual resistance of the sputtered film was higher than the residual resistance of the vapor diffused Nb_3Sn film. The higher residual resistance of the sputtered film originated from the Nb of the uncoated regions of the substrate. A picture of the measured sample is shown in Fig. 5, where the coated Nb_3Sn films and uncoated Nb substrate can be easily distinguished. RF surface resistance measurement at lower temperatures up to 2 K reported previously showed a second transition at ~8 K due to the uncoated region of the substrate [8]. Since the uncoated part of the substrate remains in the normal conducting state up to its critical temperature (9.25 K), the resistance measured is higher to 5 mΩ even though the film is in superconducting state below 17.2 K.

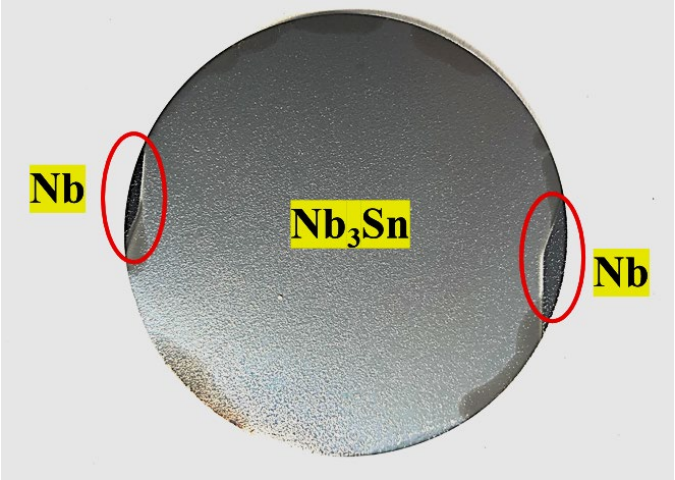

Fig. 4. Picture of the measured sample showing the uncoated region exposed to the Nb substrate.

Another possible reason for the higher residual resistance of the sputtered Nb_3Sn film could be the voids observed on the surface. The residual resistance as well as the T_c of the films can be improved by improving the film surface and stoichiometry by optimizing the coating and annealing parameters.

VI. Conclusion

Nb_3Sn films were fabricated by annealing sputtered multilayers of Nb and Sn layers at 950 °C for 3 h to study the structural, morphological, and RF superconducting properties for its application in SRF cavities. The films had a surface of tightly packed grains with randomly distributed voids and lower Sn composition than the stoichiometric Nb_3Sn. The best film had a RF superconducting transition at ~17.2 K and a residual resistance of ~5 mΩ at 12 K.

Acknowledgment

This material is based upon work supported by the U.S. Department of Energy, Office of Science, Office of Nuclear Physics under Contract No. DE-AC05-06OR23177. The authors acknowledge Drs. Michael J. Kelley, Gianluigi Ciovati for their suggestions and Dr. Uttar Pudasaini for his help with sample annealing.

References

[1] S. Posen and D. L. Hall, "Nb_3Sn superconducting radiofrequency cavities: fabrication, results, properties, and prospects", *Supercond. Sci. Technol.*, vol. 30, 2017, 033004

[2] A. M. Valente-Feliciano, "Superconducting RF materials other than bulk niobium: a review", *Supercond. Sci. and Technol.*, 2016 Sep 26; 29(11): 113002.

[3] U. Pudasaini, G. V. Eremeev, C. E. Reece, J. Tuggle, M. J. Kelley, "Initial growth of tin on niobium for vapor diffusion coating of Nb_3Sn. *Supercond. Sci. and Technol.*, 2019 Mar 1;32(4): 045008.

[4] U. Pudasaini *et al.*, "Recent Results From Nb_3Sn Single Cell Cavities Coated at Jefferson Lab", *in Proc. 19th Int. Conf. RF Superconductivity (SRF'19), Dresden, Germany*, Jun.-Jul. 2019, pp. 65-70. doi:10.18429/JACoW-SRF2019-MOP018.

[5] G. Eremeev, W. Clemens, K. Macha, C. E. Reece, A. M. Valente-Feliciano, S. Williams, U. Pudasaini, M. Kelley, "Nb_3Sn multicell cavity coating system at Jefferson Lab", *Rev. Sci. Instrum.*, 2020 Jul 1;91(7): 073911.

[6] S. Posen *et al.*, "Nb_3Sn at Fermilab: Exploring Performance", in *Proc. 19th Int. Conf. RF Superconductivity (SRF'19), Dresden, Germany*, Jun.-Jul. 2019, pp. 818-822. doi:10.18429/JACoW-SRF2019-THFUB1.

[7] E. A. Ilyina, G. Rosaz, J. B. Descarrega, W. Vollenberg, A. J. Lunt, F. Leaux, S. Calatroni, W. Venturini-Delsolaro, M. Taborelli, "Development of sputtered Nb_3Sn films on copper substrates for superconducting radiofrequency applications", *Supercond. Sci. and Technol.,* 2019 Jan 21;32(3):035002.

[8] Md. N. Sayeed *et al.*, "Deposition of Nb_3Sn Films by Multilayer Sequential Sputtering for SRF Cavity Application", *in Proc. 19th Int. Conf. RF Superconductivity (SRF'19), Dresden, Germany*, Jun.-Jul. 2019, pp. 637-641. doi:10.18429/JACoW-SRF2019-TUP079.

[9] R. Valizadeh *et al.*, "PVD Depostion of Nb_3Sn Thin Film on Copper Substrate from an Alloy Nb_3Sn Target", *in Proc. 10th Int. Particle Accelerator Conf. (IPAC'19), Melbourne, Australia*, May 2019, pp. 2818-2821. doi:10.18429/JACoW-IPAC2019-WEPRB011.

[10] M. N. Sayeed, U. Pudasaini, C. E. Reece, G. V. Eremeev, and H. E. Elsayed-Ali, "Properties of Nb_3Sn films fabricated by magnetron sputtering from a single target." *Appl. Surf. Sci.* (2020). Doi: 10.1016/j.apsusc.2020.148528.

[11] B. P. Xiao, C. E. Reece, H. L. Phillips, R. L. Geng, H. Wang, F. Marhauser, M. J. Kelley, "Note: Radio frequency surface impedance characterization system for superconducting samples at 7.5 GHz.", *Rev. Sci. Instrum.*, 2011 May 25;82(5):056104.

[12] M. N. Sayeed, U. Pudasaini, C. E. Reece, G. Eremeev, H. E. Elsayed-Ali, "Structural and superconducting properties of Nb_3Sn films grown by multilayer sequential magnetron sputtering", *J. Alloys Compd.* 2019 Sep 5;800:272-8, doi: 10.1016/j.jallcom.2019.06.017.

[13] M. N. Sayeed, U. Pudasaini, C. E. Reece, G. Eremeev, H. E. Elsayed-Ali, "Effect of layer thickness on structural, morphological and superconducting properties of Nb_3Sn films fabricated by multilayer sequential sputtering", *IOP Conf. Ser.: Mater. Sci. Eng.* 2020, 756, 012014, doi: 10.1088/1757-899X/756/1/012014.

[14] S. I. Sosa Guitron, J. R. Delayen, A. V. Gurevich, E. Chang Beom, C. Sundahl, and G. V. Eremeev, "Measurements of RF Properties of Thin Film Nb_3Sn Superconducting Multilayers Using a Calorimetric Technique", *in Proc. 17th Int. Conf. RF Superconductivity (SRF'15), Whistler, Canada*, Sep. 2015, paper TUPB060, pp. 720-722.

[15] G. V. Eremeev, H. L. Phillips, A-M. Valente-Feliciano, C. E. Reece, and B. P. Xiao, "Characterization of Superconducting Samples With SIC System for Thin Film Developments: Status and Recent Results.", *in Proc. 16th Int. Conf. RF Superconductivity (SRF'13), Paris, France*, Sep. 2013, paper TUP070, pp. 599-602.

[16] J. Halbritter, "Fortran Program for the Computation of the Surface Impedance of Superconductors", *Internal Notes KFZ Karlsruhe* 3/70-6. June 1970.

[17] A. Godeke, "A review of the properties of Nb_3Sn and their variation with A15 composition, morphology and strain state", *Supercond. Sci. Technol.*, 2006 Jun 26;19(8): R68.